



Research Paper

Quantifying changes in the bacterial thiol redox proteome during host-pathogen interaction

Kaibo Xie^a, Christina Bunse^b, Katrin Marcus^b, Lars I. Leichert^{a,*}

^a Ruhr University Bochum, Institute of Biochemistry and Pathobiochemistry, Microbial Biochemistry, 44780 Bochum, Germany

^b Ruhr University Bochum, Medizinisches Proteom-Center, 44801 Bochum, Germany



ABSTRACT

Phagocyte-derived production of a complex mixture of different oxidants is a major mechanism of the host defense against microbial intruders. On the protein level, a major target of these oxidants is the thiol group of the amino acid cysteine in proteins. Oxidation of thiol groups is a widespread regulatory post-translational protein modification. It is used by bacteria to respond to and to overcome oxidative stress. Numerous redox proteomic studies have shown that protein thiols in bacteria, such as *Escherichia coli* react towards a number of oxidants in specific ways. However, our knowledge about protein thiols in bacteria exposed to the complex mixture of oxidants encountered in the phagolysosome is still limited. In this study, we used a quantitative redox proteomic method (OxICAT) to assess the in vivo thiol oxidation status of phagocytized *E. coli*. The majority (65.5%) of identified proteins harbored thiols that were significantly oxidized (> 30%) upon phagocytosis. A substantial number of these proteins are from major metabolic pathways or are involved in cell detoxification and stress response, suggesting a systemic breakdown of the bacterial cysteine proteome in phagocytized bacteria. 16 of the oxidized proteins provide *E. coli* with a significant growth advantage in the presence of H₂O₂, when compared to deletion mutants lacking these proteins, and 11 were shown to be essential under these conditions.

1. Introduction

Neutrophils are key players of the innate immune response. In response to invading microorganisms, they are recruited to sites of infection, where they internalize pathogens into compartments called phagosomes. During the process of phagocytosis, the NADPH oxidase 2 complex (NOX2) is assembled and activated [56]. This activation of NOX2 is dependent on the phosphorylation of its subunits, which is stimulated upon phagocytosis [4,15]. As a result, superoxide anion (O₂⁻) is generated by one-electron reduction of phagosomal oxygen at the expense of cytosolic NADPH [53]. To compensate for the directional transport of electrons (e⁻) into the phagosome, protons (H⁺) are transported by voltage-gated H⁺-channels leading to acidification of the phagosomal compartment [17]. The superoxide anion O₂⁻ can disproportionate into hydrogen peroxide (H₂O₂), a reaction catalyzed by superoxide dismutase. H₂O₂ can, in turn, generate [•]OH and hypochlorous acid (HOCl). The former is generated typically through Fenton-chemistry, the latter is produced catalytically by myeloperoxidase (MPO) [44,58]. Such naturally occurring chemically reactive oxidants containing the element oxygen are often called “reactive oxygen species” (ROS).

In addition to those “ROS”, the phagosome also produces “reactive nitrogen species” (RNS), reactive oxidants containing the element nitrogen. Nitric oxide ([•]NO) is formed by the inducible nitric oxide

synthase (iNOS) [64]. [•]NO can further react with O₂⁻, generating peroxynitrite (ONOO⁻) and nitrogen dioxide ([•]NO₂). Working together, these highly reactive oxygen and nitrogen species are crucial for the effective clearance of pathogenic intruders. Mice, which lack both iNOS and NOX2 and thus can produce neither [•]NO nor O₂⁻ are therefore heavily compromised in their defense against bacteria [60].

Oxidants that are produced in the phagosome can react with and damage major cellular components of pathogens, including DNA, lipids and proteins. However, bacteria have their own mechanisms to protect themselves from oxidative stress. Antioxidant enzymes such as superoxide dismutases, catalases and peroxidases are some of the most common enzymes used by bacteria for detoxification and thus maintain the cell integrity [8].

In addition to those detoxifying enzymes, a few bacteria have evolved more specialized strategies to survive phagocytes including the pathogens *Mycobacterium tuberculosis* and *Salmonella enterica* serovar Typhimurium. Mechanisms involved in *M. tuberculosis* survival within the host cell include the inhibition of phagosome acidification and inhibition of the phagosome-lysosome fusion [43]. In comparison, intracellular *S. Typhimurium* translocate effector proteins into the host cell cytosol, alter the vesicular trafficking and modify the phagosome to their own advantage and survive in an acidified vacuole known as the “*Salmonella*-Containing Vacuole” (SCV). The biogenesis of SCV has been shown to be dependent on a type III secretion systems (T3SS) [45,62]. A

* Corresponding author.

E-mail address: lars.leichert@ruhr-uni-bochum.de (L.I. Leichert).

<https://doi.org/10.1016/j.redox.2018.101087>

Received 18 October 2018; Received in revised form 13 December 2018; Accepted 18 December 2018

Available online 19 December 2018

2213-2317/ © 2018 The Authors. Published by Elsevier B.V. This is an open access article under the CC BY license (<http://creativecommons.org/licenses/by/4.0/>).

specific set of T3SS effectors has been shown to be directly involved in oxidative stress evasion strategies [27].

However, most bacteria are rapidly killed, once caught in the phagosome of neutrophils [69]. The mechanism, by which host-derived oxidants kill bacteria, is still not fully understood. On the protein level, a major target of oxidants is the thiol group of the amino acid cysteine. As is well known, the cysteine residue is used to keep conformational rigidity of structural proteins via the formation of disulfide bonds. However, within the cytosol of a cell, biological pathways often require catalytically active cysteines [52]. During the last few years, an increasing number of proteins involved in cellular stress response have been identified that are functionally regulated by reversible thiol oxidation including chaperones and transcription factors [21,32,71]. As shown by numerous studies, protein thiols in bacteria react towards a number of oxidants in a specific way [5,37,39]. However, the thiol redox proteome in bacteria that have encountered the complex mixture of phagosomal oxidants has not yet been investigated.

In this study, we established a method to separate phagocytized *E. coli* from extracellular *E. coli* after coinoculation with the PLB-985 neutrophil-like cell line. Using a thiol trapping technique termed OxICAT, we then quantified the redox proteome of both the intracellular and extracellular *E. coli*. When compared to *E. coli* that were outside of the neutrophils and thus did not experience phagocytosis, 65.5% of the proteins identified in phagocytized *E. coli* showed an increase in cysteine oxidation of greater than 30%. The oxidized proteins were part of protein, nucleotide and carbohydrate metabolic pathways but were also involved in cell detoxification and stress response, which indicate a systemic oxidation of protein thiols. This suggests a total break-down of *E. coli*'s thiol proteome after encountering neutrophil phagocytosis. Moreover, as revealed by subsequent growth rate assays, 16 mutants, which lack proteins identified in our redox proteomic experiments, showed increased sensitivity towards oxidative stress. 11 of the genes encoding those proteins were essential for the growth of *E. coli* under otherwise sublethal oxidative stress conditions.

2. Experimental procedures

2.1. PLB-985 cell culture and differentiation

The human myeloid leukemia cell line PLB-985 (DSMZ, German collection of microorganisms and cell culture) was cultured in RPMI 1640 medium supplemented with 10% heat-inactivated fetal bovine serum (FBS), 1% GlutaMAX (Life Technologies, Darmstadt, Germany) at 37 °C, in a humidified atmosphere of 5% CO₂ and passaged twice weekly. For granulocytic differentiation of cells, exponentially growing cells at a density of 2 × 10⁵/ml were cultured in RPMI 1640 medium supplemented with 10% FCS, 1% GlutaMAX and 1.25% DMSO for five days. On day four, cells were stimulated with 2000 U/ml interferon-γ (IFN-γ) [18,51].

2.2. Phagocytosis of bacteria by PLB-985 cells

A culture of *E. coli* AM39 harbouring a generated vector containing roGFP2-Orp1 (for bacterial strains used in this study see Table 1) was grown to an OD₆₀₀ of 0.4 at 37 °C with 100 µg/ml ampicillin. 100 µM IPTG was added to allow roGFP2-Orp1 expression overnight at 20 °C. The bacterial cells were washed twice in PBS (pH 7.4) and opsonized with 5 mg/ml human immunoglobulin G (hIgG, Sigma-Aldrich, St. Louis, MO) for 30 min at 37 °C. Afterwards, bacteria were washed twice with PBS and resuspended in PBS supplemented with 0.5% FBS to an OD₆₀₀ of 0.1 (10⁸ cells/ml), unless described differently. Differentiated PLB-985 cells were washed once with PBS, resuspended in PBS supplemented with 0.5% FBS to a concentration of 10⁷ cells/ml and mixed with opsonized *E. coli* in the same volume (multiplicity of infection, MOI = 10). The cell suspension consisting of PLB-cells and *E. coli* was coinoculated at 37 °C for 2 h.

Table 1
Bacterial strains used in this study.

Strain	Genotype	Source or reference
<i>E. coli</i> AM39	<i>E. coli</i> MG1655 (K-12 F ⁺ λ: <i>ibvG^r rfb-50 rph-1</i>) transformed with the roGFP2-Orp1 containing plasmid pCC _{roGFP2-orp1}	[14] ^a
<i>E. coli</i> BW25113	<i>lacI</i> ⁺ <i>rrnB</i> _{T14} <i>ΔlacZ</i> _{WJ16} <i>hsdR</i> 514 <i>ΔaraBAD</i> _{AH33} <i>ΔrhaBAD</i> _{LD78} <i>rph-1</i> Δ(<i>araB-D</i>)567 Δ(<i>rhaD-B</i>)568 <i>ΔlacZ</i> 4787(:: <i>rrnB-3</i>) <i>hsdR</i> 514 <i>rph-1</i>	The National BioResource Project (National Institute of Genomics, Japan) ^b
<i>E. coli</i> JW3975	<i>E. coli</i> BW25113 <i>ΔaceA</i>	See above ^b
<i>E. coli</i> JW3974	<i>E. coli</i> BW25113 <i>ΔaceB</i>	See above ^b
<i>E. coli</i> JW2293	<i>E. coli</i> BW25113 <i>ΔackA</i>	See above ^b
<i>E. coli</i> JW0911	<i>E. coli</i> BW25113 <i>ΔaspC</i>	See above ^b
<i>E. coli</i> JW1737	<i>E. coli</i> BW25113 <i>ΔastC</i>	See above ^b
<i>E. coli</i> JW3712	<i>E. coli</i> BW25113 <i>ΔatpA</i>	See above ^b
<i>E. coli</i> JW5702	<i>E. coli</i> BW25113 <i>Δcrp</i>	See above ^b
<i>E. coli</i> JW4346	<i>E. coli</i> BW25113 <i>ΔdeoB</i>	See above ^b
<i>E. coli</i> JW2077	<i>E. coli</i> BW25113 <i>ΔgatB</i>	See above ^b
<i>E. coli</i> JW2873	<i>E. coli</i> BW25113 <i>ΔgcvT</i>	See above ^b
<i>E. coli</i> JW3389	<i>E. coli</i> BW25113 <i>ΔglpD</i>	See above ^b
<i>E. coli</i> JW3897	<i>E. coli</i> BW25113 <i>ΔglpK</i>	See above ^b
<i>E. coli</i> JW0710	<i>E. coli</i> BW25113 <i>ΔgltA</i>	See above ^b
<i>E. coli</i> JW3179	<i>E. coli</i> BW25113 <i>ΔgltB</i>	See above ^b
<i>E. coli</i> JW2011	<i>E. coli</i> BW25113 <i>Δgnd</i>	See above ^b
<i>E. coli</i> JW4103	<i>E. coli</i> BW25113 <i>ΔgroL</i>	See above ^b
<i>E. coli</i> JW5401	<i>E. coli</i> BW25113 <i>ΔguaB</i>	See above ^b
<i>E. coli</i> JW1122	<i>E. coli</i> BW25113 <i>Δicd</i>	See above ^b
<i>E. coli</i> JW3747	<i>E. coli</i> BW25113 <i>ΔilvC</i>	See above ^b
<i>E. coli</i> JW3592	<i>E. coli</i> BW25113 <i>Δkbl</i>	See above ^b
<i>E. coli</i> JW0336	<i>E. coli</i> BW25113 <i>ΔlacI</i>	See above ^b
<i>E. coli</i> JW0112	<i>E. coli</i> BW25113 <i>Δlpd</i>	See above ^b
<i>E. coli</i> JW0872	<i>E. coli</i> BW25113 <i>Δltp</i>	See above ^b
<i>E. coli</i> JW2662	<i>E. coli</i> BW25113 <i>ΔluxS</i>	See above ^b
<i>E. coli</i> JW2447	<i>E. coli</i> BW25113 <i>ΔmaeB</i>	See above ^b
<i>E. coli</i> JW3205	<i>E. coli</i> BW25113 <i>Δmdh</i>	See above ^b
<i>E. coli</i> JW3194	<i>E. coli</i> BW25113 <i>Δnana</i>	See above ^b
<i>E. coli</i> JW2502	<i>E. coli</i> BW25113 <i>Δndk</i>	See above ^b
<i>E. coli</i> JW2279	<i>E. coli</i> BW25113 <i>ΔnuoF</i>	See above ^b
<i>E. coli</i> JW3933	<i>E. coli</i> BW25113 <i>ΔoxyR</i>	See above ^b
<i>E. coli</i> JW5300	<i>E. coli</i> BW25113 <i>ΔproQ</i>	See above ^b
<i>E. coli</i> JW0325	<i>E. coli</i> BW25113 <i>ΔprpD</i>	See above ^b
<i>E. coli</i> JW2409	<i>E. coli</i> BW25113 <i>ΔptsI</i>	See above ^b
<i>E. coli</i> JW1843	<i>E. coli</i> BW25113 <i>ΔpykA</i>	See above ^b
<i>E. coli</i> JW4205	<i>E. coli</i> BW25113 <i>ΔpyrI</i>	See above ^b
<i>E. coli</i> JW3907	<i>E. coli</i> BW25113 <i>ΔrpmE</i>	See above ^b
<i>E. coli</i> JW3037	<i>E. coli</i> BW25113 <i>ΔtrpS</i>	See above ^b
<i>E. coli</i> JW0713	<i>E. coli</i> BW25113 <i>ΔsdhA</i>	See above ^b
<i>E. coli</i> JW0714	<i>E. coli</i> BW25113 <i>ΔsdhB</i>	See above ^b
<i>E. coli</i> JW0717	<i>E. coli</i> BW25113 <i>ΔsucC</i>	See above ^b
<i>E. coli</i> JW0718	<i>E. coli</i> BW25113 <i>ΔsucD</i>	See above ^b
<i>E. coli</i> JW0396	<i>E. coli</i> BW25113 <i>Δtgt</i>	See above ^b
<i>E. coli</i> JW5478	<i>E. coli</i> BW25113 <i>ΔtktA</i>	See above ^b
<i>E. coli</i> JW3686	<i>E. coli</i> BW25113 <i>ΔtnaA</i>	See above ^b
<i>E. coli</i> JW1317	<i>E. coli</i> BW25113 <i>Δtpx</i>	See above ^b
<i>E. coli</i> JW1254	<i>E. coli</i> BW25113 <i>ΔtrpC</i>	See above ^b
<i>E. coli</i> JW3943	<i>E. coli</i> BW25113 <i>ΔtufB</i>	See above ^b
<i>E. coli</i> JW5394	<i>E. coli</i> BW25113 <i>ΔucpA</i>	See above ^b
<i>E. coli</i> JW1370	<i>E. coli</i> BW25113 <i>ΔuspF</i>	See above ^b
<i>E. coli</i> JW3063	<i>E. coli</i> BW25113 <i>ΔuxaC</i>	See above ^b
<i>E. coli</i> JW5126	<i>E. coli</i> BW25113 <i>ΔycbX</i>	See above ^b
<i>E. coli</i> JW1194	<i>E. coli</i> BW25113 <i>ΔychF</i>	See above ^b
<i>E. coli</i> JW1772	<i>E. coli</i> BW25113 <i>ΔyeaG</i>	See above ^b
<i>E. coli</i> JW2518	<i>E. coli</i> BW25113 <i>ΔyfhR</i>	See above ^b
<i>E. coli</i> JW2568	<i>E. coli</i> BW25113 <i>ΔyfiQ</i>	See above ^b
<i>E. coli</i> JW2647	<i>E. coli</i> BW25113 <i>ΔygaM</i>	See above ^b
<i>E. coli</i> JW2647	<i>E. coli</i> BW25113 <i>ΔygaM</i>	See above ^b
<i>E. coli</i> JW3040	<i>E. coli</i> BW25113 <i>Δygf</i>	See above ^b

^a Degrossoli et al. [14].

^b Baba et al. [2].

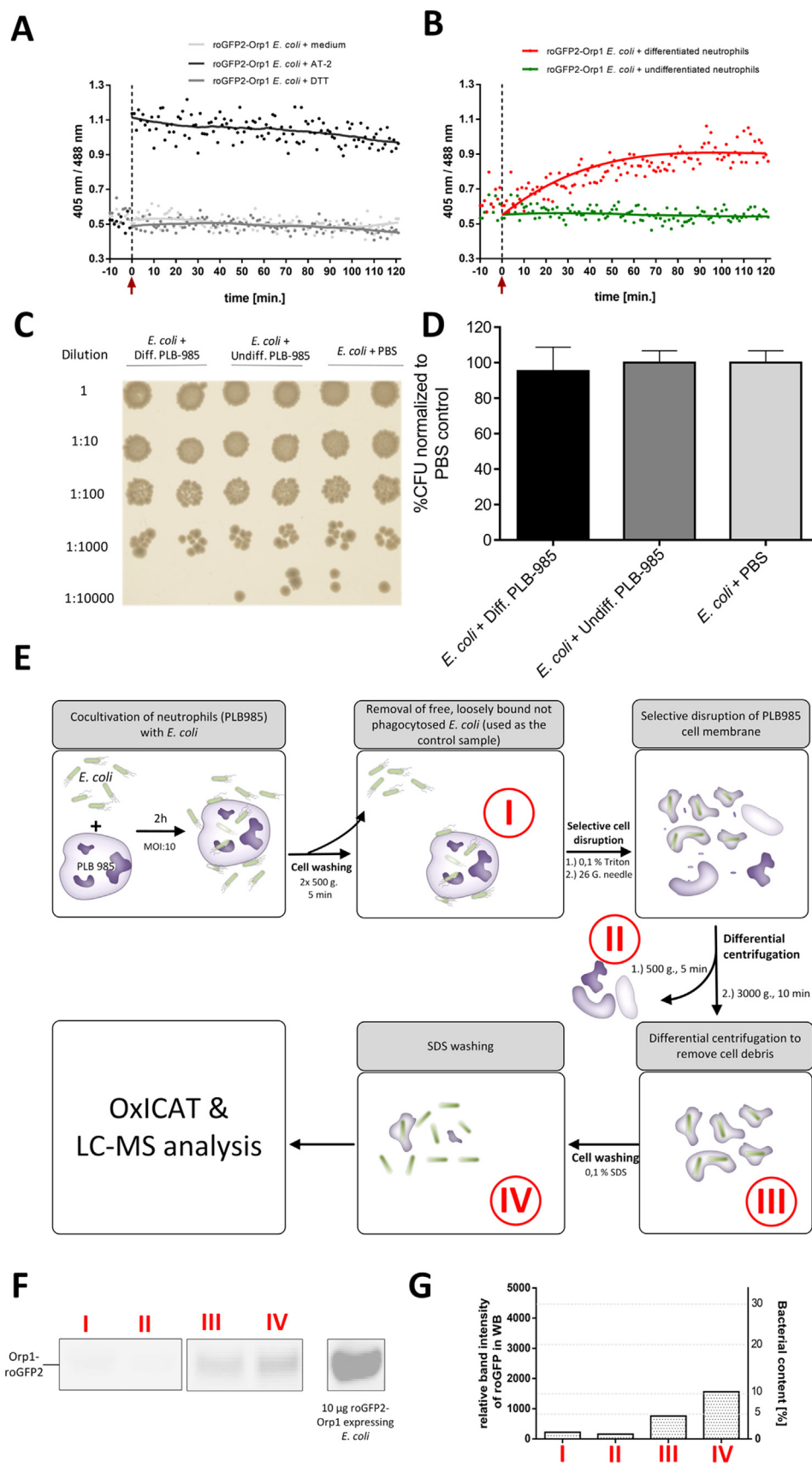


Fig. 1. Effects of phagocytosis by neutrophil-like PLB-985 cells on *E. coli* and enrichment of phagocytized bacteria. **A.** roGFP2-Orp1 expressing *E. coli* were mixed with 50 mM dithiothreitol (DTT), 1 mM aldrithiol-2 (AT-2) or **B.** neutrophil-like, differentiated PLB-985 cells (MOI (multiplicity of infection): ten *E. coli* to one PLB-985) as indicated by the red arrow. The redox state of roGFP2-orp1 was tracked for 120 min by measuring fluorescence intensities at 510 nm for both excitation wavelengths 488 nm and 405 nm. Once mixed with differentiated PLB cells, the redox-ratio of roGFP2-Orp1 expressing *E. coli* cells increased from 0.6 to 1.0 in a time-dependent manner and reached its maximum after approximately 80 min. **C.** Serial dilutions of co-incubation assays (MOI: 2:10, 2 h of co-incubation) were plated on LB bacterial medium plates to determine killing by phagocytosis. **D.** No significant decrease in colony forming units (cfu) through action of differentiated PLB-985 was observed, when compared to undifferentiated PLB-985 cells or PBS, which served as control. **E.** Separation of phagocytized bacteria and non-phagocytized bacteria incubated with PLB-985 cells (MOI 10:1, I). Host cells were disrupted mechanically and centrifuged at 500 g to remove cell debris (II). Supernatant was centrifuged at 3000 g to collect the bacterial fraction (III), which was washed with 0.1% SDS (IV). Respective fractions taken for western blot are indicated by the roman numerals. **F.** & **G.** Western Blot of a normalized SDS-PAGE probed with α -GFP antibody (10 µg total protein per lane). Relative *E. coli* amount was determined by comparing the relative band intensity of roGFP2-Orp1 of each fraction to a known amount of lysate of *E. coli* from the same batch.

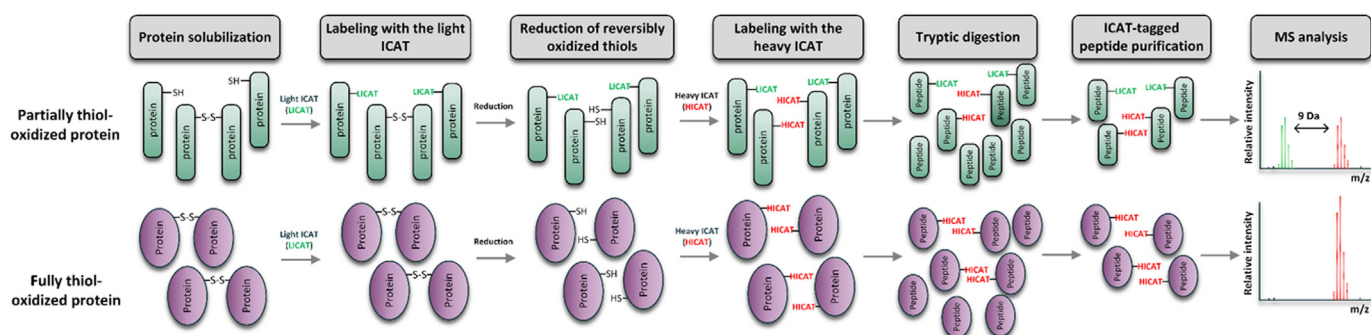


Fig. 2. Quantification of thiol-oxidation using OxICAT. First, proteins of interest are solubilized and denatured, which allows the reaction of the isotopically light ¹²C-ICAT reagent (LICAT, green) with all free cysteines. Second, reversibly oxidized cysteines are reduced using Tris(2-carboxyethyl)phosphine and labeled with the isotopically heavy ¹³C-ICAT (HICAT, red). Then, the protein mixture is digested by trypsin and the ICAT-tagged peptides are purified using the biotin tag. Finally, the peptide mixture is analyzed using mass spectrometry. Partially thiol-oxidized proteins are labeled with both the LICAT and the HICAT. Fully oxidized thiol-oxidized proteins are labeled with HICAT only. The relative oxidation of a cysteine is reflected by the proportion of its respective LICAT- and HICAT-labeling.

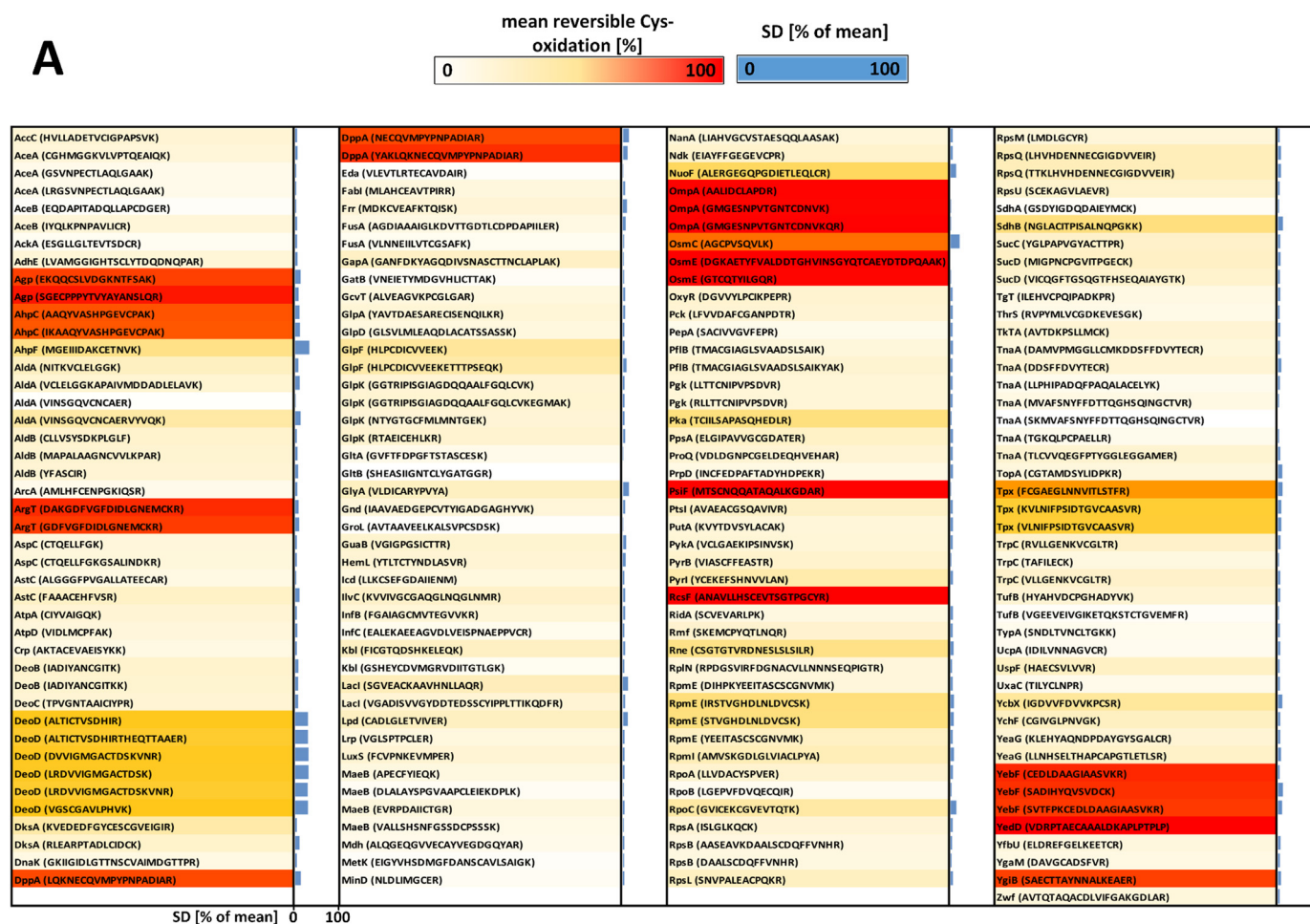


Fig. 3. Relative thiol oxidation of 173 identified cysteine-containing peptides in *E. coli* cells during phagocytosis. *E. coli* cells were incubated with neutrophils for 2 h. Extracellular *E. coli* cells were separated from the neutrophils and the intracellular *E. coli* cells enriched thereafter. Both the extracellular (A) and the intracellular (B) *E. coli* cells were analyzed using OxICAT. The relative thiol oxidation of 173 matched cysteine residues were visualized using heat maps based on data shown in Supplementary Table 1. The white-yellow-red gradient denotes 0–100% oxidation. The standard deviation (SD) of three biological replicates is shown in blue.

2.3. Real-time analysis of roGFP2-Orp1 oxidation state in *E. coli*

The measurement of roGFP2-Orp1 oxidation during the coinubation with PLB-985 cells was done in a 96-well format as described previously [14]. In short, 50 μl of *E. coli* expressing roGFP2-Orp1 at a final OD₆₀₀ of 0.1 were either mixed with 50 μl of PLB-985 cells at a

final concentration of 10⁷ cells/ml or with the respective reagents in a 96-well plate (Nunc black, clear-bottom, Rochester, NY). The fluorescence intensity was measured every minute for 2 h at the excitation wavelength 405 nm and 488 nm and the emission wavelength 510 nm. The 405/488 nm ratio was calculated using Excel 2016 (Microsoft, Redmond, WA) and visualized using GraphPad Prism (version 6.01,

B

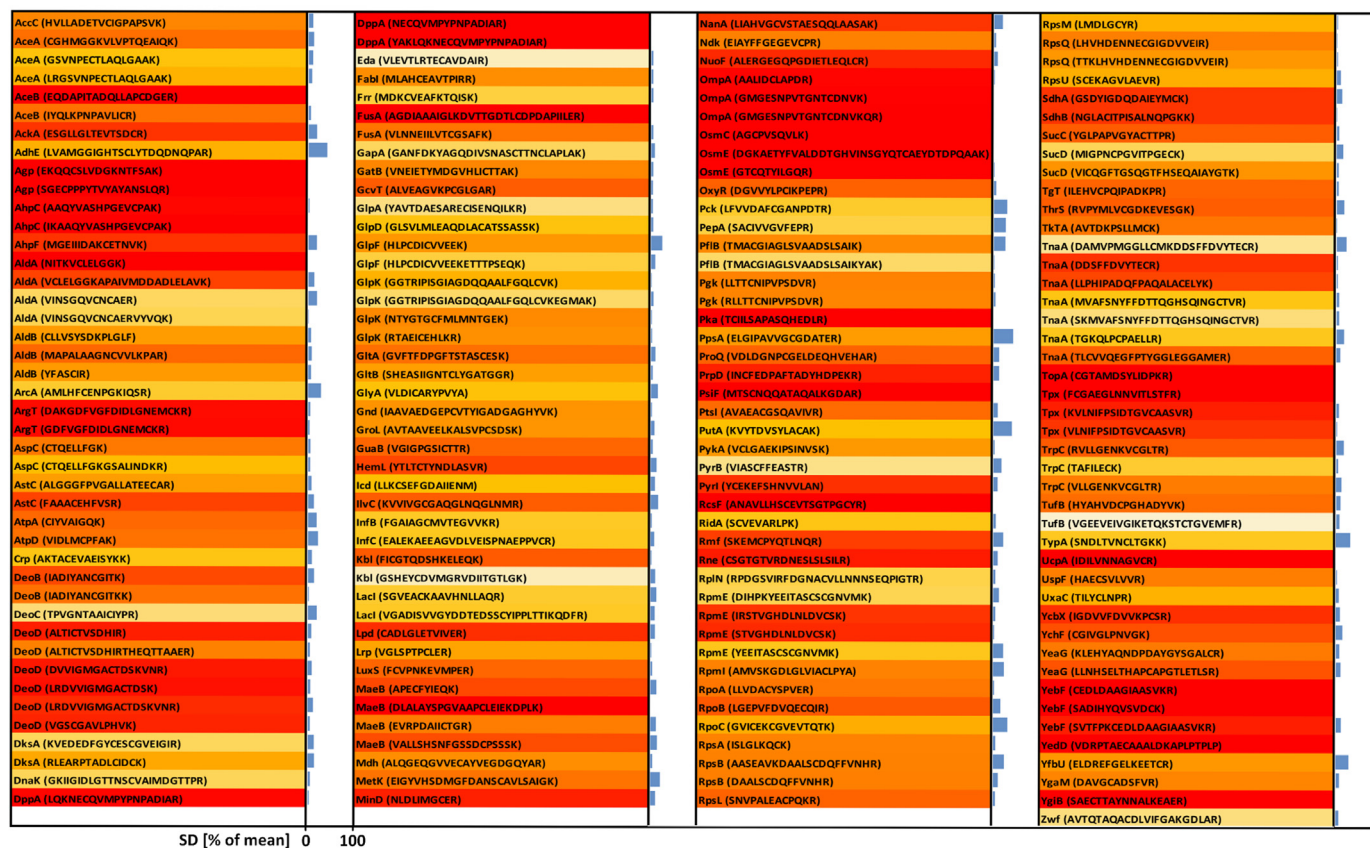


Fig. 3. (continued)

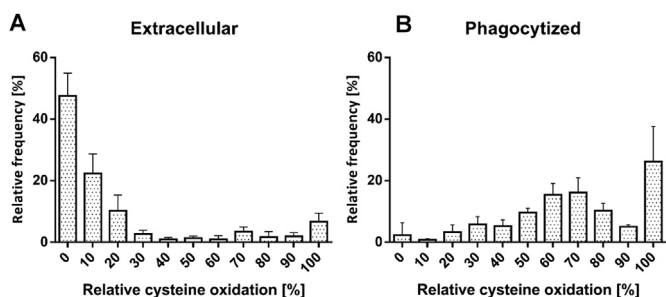


Fig. 4. Frequency distribution of the relative thiol oxidation of the identified cysteine-containing peptides in *E. coli* cells during phagocytosis. *E. coli* cells were incubated with neutrophils for 2 h. Extracellular *E. coli* cells were separated from the neutrophils and the intracellular *E. coli* cells enriched thereafter. Both the extracellular (A) and the phagocytized (B) *E. coli* cells were analyzed using OxICAT. The relative thiol oxidation of 173 matched cysteine residues were visualized using frequency distribution analysis.

GraphPad, San Diego, CA).

2.4. Fractionation of phagocytized and non-phagocytized bacteria

Differentiated PLB-985 cells were co-cultivated with bacteria as described above for 2 h. Afterwards, the PLB cells were washed twice with ice-cold PBS in order to remove extracellular bacteria (500 g, 5 min, 4 °C), the resulting supernatant containing non-phagocytized bacteria was used as the control sample for subsequent OxICAT-analysis. The resulting pellet was resuspended in 0.1% Triton (v/v) and passed five times through a 26-G needle in order to lyse the PLB-cells. Cell nuclei and large debris were removed by low-speed centrifugation

(500 g, 5 min, 4 °C). The bacteria in the supernatant were recovered by following mid-speed centrifugation (3000 g, 10 min, 4 °C). The bacteria-containing pellet was rinsed once with 0.1% SDS (w/v) and pelleted (16.000 g, 5 min, 4 °C). This bacterial fraction was then immediately used for further analysis. The extracellular control obtained from the supernatant of the initial centrifugation (see above) was passed through a 26-G needle and treated with 0.1% Triton and SDS as well. This whole enrichment procedure was carried out in less than 45 min. Protein concentrations were determined using the Pierce™ BCA Protein Assay Kit (Thermo Scientific, Waltham, MA) and the relative bacterial protein content was monitored with Western Blot analysis using an antibody against GFP (1:4000, rabbit, Sigma-Aldrich), which was reactive to roGFP2-Orp1 expressed by *E. coli*.

2.5. SDS-PAGE and Western Blot

Protein samples were separated on 4–12% Bis-Tris Gels (NuPAGE™, Invitrogen, Carlsbad, CA) under reducing conditions (200 V, 40 min). For Western Blot analysis, proteins were transferred onto nitrocellulose membranes using the iBlot™ 2 Dry Blotting System (Invitrogen). Membranes were probed with antibodies against GFP (rabbit, 1:4000, Thermo Fisher Scientific). Proteins of interest were detected with fluorescent anti-rabbit antibody (goat, 1:10000, IRDye 680RD, LICOR, NE). Blots were imaged with an infrared imaging system (Odyssey Classic, LICOR, NE) using a three minute exposure time. Band intensity was determined using ImageJ [55].

2.6. OxICAT labeling of protein extracts

The OxICAT analysis was done according to the protocol of Lindemann and Leichert [37,38]. Briefly, protein labeling was done

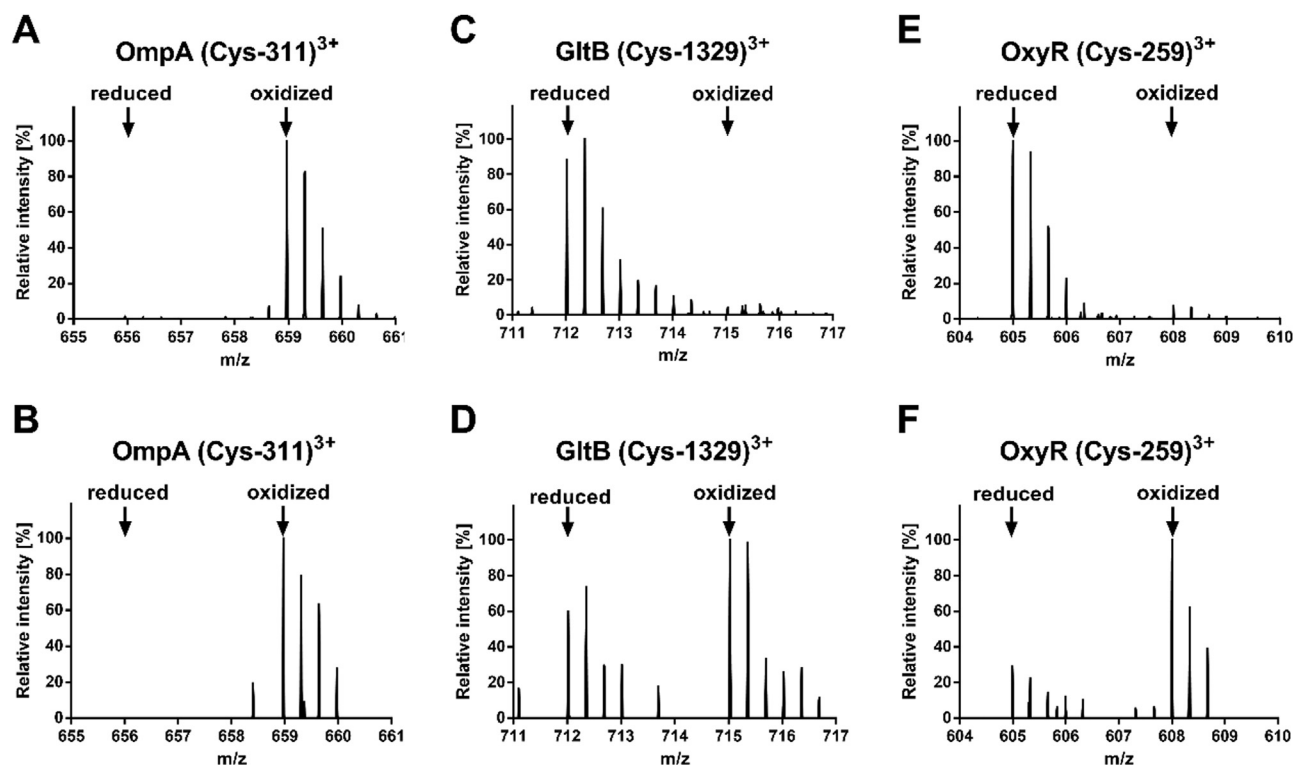


Fig. 5. MS-spectra of selected ICAT-labeled cytoplasmic and periplasmic protein thiols in extracellular and phagocytized *E. coli*. *E. coli* cells were co-incubated with a neutrophil like human cell line (PLB-985) at 37 °C for 2 h to allow phagocytosis. Protein thiols of both extracellular and phagocytized *E. coli* cells were enriched and differentially labeled with OxICAT. Mass signals of peptides labeled with the ^{12}C -ICAT (reduced) and ^{13}C -ICAT (oxidized) are shown. Cysteine 311 from the periplasmic protein OmpA was fully oxidized in both extracellular and phagocytized *E. coli* cells (A, B). Cysteine 1329 from the cytoplasmic protein GltB was predominantly reduced in extracellular *E. coli* cells and partially oxidized during phagocytosis (C, D). Cysteine 259 of OxyR was found more oxidized during phagocytosis as well (E, F).

using reagents provided by the Cleavable ICAT Method Development kit and Bulk kit (AB SCIEX, Framingham, MA). 100 μg of proteins were dissolved with one vial of the light-labeled ICAT predissolved in a mixture consisting of 80 μl DAB-buffer (6 M Urea, 200 mM Tris-HCl, 0.5% SDS, 10 mM EDTA, pH 8.5) and 20 μl acetonitrile (ACN), incubated for 2 h at 37 °C in the dark. Proteins from this solution were precipitated overnight at -20 °C with 80% acetone, rinsed twice with 1 ml of 80% acetone each and collected as pellet (4 °C, 16,000 g, 30 min). The pellet was dried at 37 °C for 5 min, dissolved in 80 μl DAB buffer containing 1 mM tris(2-carboxyethyl)phosphine hydrochloride (TCEP) and incubated for 10 min at 37 °C. This solution was mixed with one vial of the heavy-labeled ICAT resuspended in 20 μl ACN. This protein solution was incubated for 2 h at 37 °C in low-light conditions. Proteins were precipitated using acetone and rinsed as described. The resulting pellet was dissolved in 80 μl of Denaturing Buffer (50 mM Tris, 0.1% SDS) from the ICAT kits as mentioned above and mixed with 20 μl ACN and 100 μl of 0.125 $\mu\text{g}/\mu\text{l}$ trypsin solution and incubated overnight at 37 °C. Subsequent peptide purification by cation exchange, avidin affinity chromatography and cleavage of the biotin-tag were performed according to the manufacturer's instructions with the modification that the Affinity Buffer-Elute (30% ACN, 0.1% TFA (trifluoroacetic acid)) was freshly prepared at the day of experiment. Purified peptides were concentrated to dryness and dissolved in 0.1% TFA for LC-MS/MS analysis.

2.7. LC-MS/MS analysis

ICAT-labeled peptides were loaded onto a reverse phase nano-LC and detected by MS/MS in an LTQ Orbitrap Elite instrument (Thermo Fisher Scientific) as described [39]. In short, samples were loaded onto a C18 precolumn (100- μm \times 2-mm Acclaim PepMap100, 5 μM , Thermo

Fisher Scientific) with 0.1% TFA with 2.5% ACN (v/v) at a flow rate of 30 $\mu\text{l}/\text{min}$ for 7 min. The peptides were then loaded onto the main column (75- μm \times 50-cm Acclaim PepMap100 C18, 3 μm , 100- \AA , Thermo Fisher Scientific) with 95% solvent A (0.1% formic acid (v/v)) and 5% solvent B (0.1% formic acid, 84% ACN (v/v)) at a flow rate of 0.4 $\mu\text{l}/\text{min}$. Subsequent elution was performed with a linear gradient of 5–40% B (120 min, 0.4 $\mu\text{l}/\text{min}$). The 6–20 most intense peaks were selected for MS/MS fragmentation (charge range +2 to +4, exclusion list size: 500, exclusion duration: 35 s, collision energy: 35 eV). The mass spectrometry proteomics raw data have been deposited to the ProteomeXchange Consortium [65] via the PRIDE partner repository with the dataset identifier [PXD011386](https://doi.org/10.26434/chemrxiv-2019-01-10).

2.8. Quantification of cysteine oxidation using Maxquant

The MaxQuant software (version 1.5.1.0, DE) [12] was used to quantify the ICAT-labeled peptide thiols. For the search engine Andromeda, the *E. coli* K12 proteome database (taxonomy ID 83333) obtained from UniProt (4323 proteins, released September 2017, The UniProt Consortium, 2017) was used. For the Andromeda search, two miscleavages were allowed, Oxidation (M) was chosen as variable modification. The parent ion mass tolerance was set to 10 ppm, the fragment ion mass tolerance set to 0.5 Da. The oxidation of each identified peptide thiol and the relative oxidation change as compared to control samples were calculated from three biological replicates using the MaxQuant analysis. Identified peptides and their respective ICAT-quantification were assessed using the "peptides.txt" MaxQuant output file. In short, "peptides.txt" was imported into Excel 2016 (Microsoft). Then, values of each identified peptide from the column "Intensity H" was divided by the respective value from the column "Intensity" and multiplied by 100. This value equals the percentage of

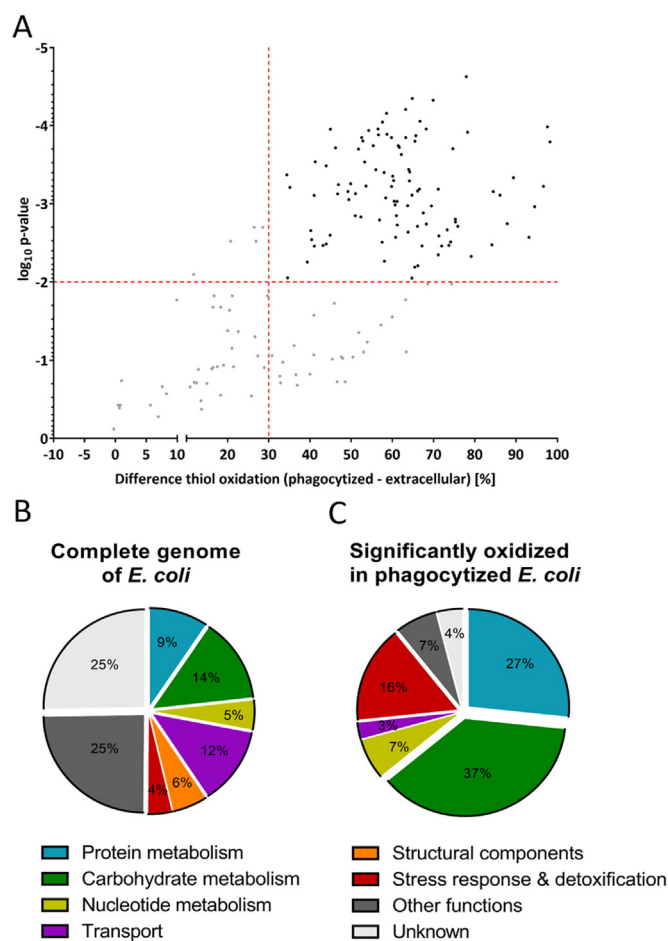


Fig. 6. Differentially oxidized protein cysteine residues of phagocytized *E. coli* and their functional classification. A. A volcano plot shows the difference of thiol oxidation, as determined by OxICAT, between *E. coli* cells, which experienced host neutrophil phagocytosis to extracellular bacteria. \log_{10} of p-values from the Student's t-distribution is plotted against the difference in thiol oxidation. The non-axial vertical line denotes an increase of 30% thiol oxidation while the non-axial horizontal line denotes a p-value of 0.01. Cysteine-containing peptides below these thresholds are shown as gray dots, peptides crossing the thresholds as black dots. B. All predicted proteins from *E. coli* K12 MG1655 (ecogene.org,16.05.2018) and their respective cellular functions. C. 76 Significantly thiol-oxidized proteins (difference > 30%; $p > 0.01$) and their respective cellular functions. Proteins involved in stress response, cell detoxification, carbohydrate and protein metabolism are overrepresented in our dataset.

reversibly oxidized cysteine of the identified peptide and was used to determine cysteine oxidation in all samples. For further analysis, column bar diagram, volcano plot and heat map were generated using GraphPad Prism (version 6.01) and Microsoft Excel 2016. MaxQuant result files and the Excel result table can be accessed at the ProteomeXchange Consortium via the PRIDE partner repository under the dataset identifier [PXD011386](https://proteomecentral.proteomexchange.org/protein/Data/PXD011386).

2.9. Bioinformatic data analysis

For the evaluation of conserved cysteines from OxICAT-identified proteins, the ConSurf server (www.consurf.tau.ac.il/2016/) was used [1]. HMMER [16] was used to obtain homologous sequences from the UNIREF-90 database (April, the 11th, 2018) with a E-value cutoff of 0.0001 and a maximum % identity between sequences of 95% and a respective minimum % identity of 35%. The top 150 sequences were retrieved for each protein and aligned using MAFFT-L-INS-I [34]. To calculate the relative surface accessibility of the identified cysteines,

NetSurfP (www.cbs.dtu.dk/services/NetSurfP/) was used [50].

2.10. Hydrogen peroxide growth inhibition assay

E. coli BW25113 as well as deletion strains used (Table 1) were obtained from the Keio collection (National Bio Resource Project, NIG, Japan) [2]. All strains were grown in LB-medium at 37 °C. At mid-logarithmic phase, bacteria cultures were split and diluted with LB-medium to a final OD_{600} of 0.03 and an H_2O_2 concentration of 2.5 mM or without H_2O_2 as a control. OD_{600} was measured every 30 min for up to 810 min at 37 °C. For quantification of the relative growth inhibition, the time for each strain to reach an OD_{600} of 0.2 was taken. For exact calculation, growth curves were fitted using third degree polynomials and the respective time was calculated from the fitted equation at OD_{600} of 0.2. The calculated values of each strain to reach an OD_{600} of 0.2 in the presence of hydrogen peroxide ($T_{H_2O_2}$) was divided by the time of the respective strain to reach the same OD in the absence of H_2O_2 ($T_{control}$). To enable comparison between strains, the relative growth inhibition was then normalized to the growth of WT bacteria, which was set to 1. For strains that did not reach an OD_{600} of 0.2 during the 810 min time course, $T_{H_2O_2}$ was set to 840 min, as this would be the earliest time point they could have reached an OD of 0.2. For those strains, $T_{H_2O_2}$ was used to determine the respective standard deviation and significance relative to the WT strain. Since the minimal relative growth inhibition calculated for these strains in this way was > 4, the relative growth inhibition was set to 4.

3. Results & discussion

3.1. Analysis and quantification of the *E. coli* thiol redox proteome in neutrophil cells by OxICAT

Professional phagocytic immune cells produce a toxic mixture of different oxidative species to counteract against pathogenic intruders like bacteria. Recently we showed that the genetically encoded fluorescent redox probe roGFP2-Orp1 is promptly oxidized in bacteria that are phagocytized by neutrophils [14]. This suggested to us that *E. coli* is under significant oxidative stress once caught in the phagolysosome. The amino acid cysteine is a well-known target of oxidants produced in the phagolysosome of neutrophils [67,69]. In our study, we were interested in analyzing the effect of oxidative stress on thiol redox proteome of *E. coli* having encountered host neutrophil phagocytosis. In order to find an optimal time point to harvest the cells for subsequent redox proteomic analysis, a 96-well format-based plate reader assay was used to monitor the oxidation state of roGFP2-Orp1 in the *E. coli* population over a time course of 2 h, while they were co-incubated with neutrophil-like PLB-985 cells. The oxidation state of roGFP2-Orp1 increased gradually, reaching a steady level after about 80 min of incubation and remained in an oxidized state until the end of the measurement (Fig. 1A and B). Nevertheless, bacteria were still fully viable when we plated serial dilutions of our co-incubation assay on LB medium after 2 h, demonstrating that probe oxidation is not caused by cell lysis (Fig. 1C and D). Thus, we decided to enrich intracellular bacteria after 2 h of co-incubation with PLB-985 cells, where the oxidation of roGFP2 in the cytoplasm of *E. coli* reached a steady level. For the subsequent redox proteomic

analysis, extracellular *E. coli* that were not phagocytized by PLB-985 were separated and served in this study as control. Due to the overwhelming amount of host cell proteins mixed with bacterial proteins [70], the development of a method to decrease the relative proportion of host cell proteins was necessary for the identification of bacterial proteins in LC-MS analysis. Several proteomic studies of bacterial pathogens upon interactions with host cells have been published. In these studies, differential centrifugation was widely used to enrich intracellular bacteria [41,59,70]. Based on those studies, we combined selective disruption of the host cell membrane, using 0.1% Triton X-100

Gene	Sequence	Identified Cysteine	Ø Control Cys-Oxidation [%]	Control SD [%]	Ø Treated Cys-Oxidation [%]	Treated SD [%]	ΔCys-Oxidation ØTreated-ØControl [%]	p-value t-test	Average ^{cell} copies/cell	Surface accessibility of identified cysteine [%]	Cys-conservation (1-9)	Description
Carbohydrate metabolism												
accA	HVLLADMETVCGIPAPSK	Cys-50	8.41	3.88	65.30	9.93	56.88	1.6E-03	4823	19	1	acetyl-CoA carboxylase, biotin carboxylase subunit
aceA	CGHMSGGVLPVPTQEAQK	Cys-195	7.42	5.77	71.21	11.71	63.79	2.3E-03	11406	15.6	9	isocitrate lyase
	LRGSAVPECTLADLGAAK	Cys-43	4.41	2.39	53.64	6.96	49.23	6.5E-04	11406	27.6	1	
	GSVNPECTLAOLGAAK	Cys-43	4.16	2.25	48.11	9.62	43.95	9.3E-03	11406	27.6	1	
aceB	EODAPITADQLLAPCDGER	Cys-409	1.76	2.49	100.00	0.00	98.24	1.6E-04	1151	22.3	3	malate synthase A
	IVQLKPNPVLVLCR	Cys-165	7.42	3.82	70.65	4.99	63.23	1.4E-04	1151	3	6	
ackA	ESGLVLEEDVTSDCR	Cys-286	3.26	3.76	100.00	0.00	96.74	3.3E-03	13696	9.4	7	acetate kinase A and propionate kinase 2
aldA	NITKVCLELGGK	Cys-249	12.14	7.47	100.00	0.00	87.86	1.8E-03	13414	6.9	6	aldehyde dehydrogenase A, NAD-linked
	VCLLEGKAPAVMDDADELAWK	Cys-249	8.67	10.09	82.82	12.91	74.14	3.1E-03	13414	6.9	6	
aldB	MAPALAGNCVWPKAPR	Cys-190	9.13	5.31	73.27	7.06	64.13	5.1E-04	8	3.4	8	aldehyde dehydrogenase B
	YFASGR	Cys-137	8.80	6.37	59.78	6.62	50.98	1.4E-03	8	7.1	2	
	CLLYVSDYKPLGLF	Cys-499	9.62	3.47	59.50	6.11	49.88	8	11.6	6		
atpA	CYVIAQK	Cys-193	8.42	3.02	73.14	19.00	64.72	8.9E-03	19988	4.7	9	F1 sector of membrane-bound ATP synthase, alpha subunit
fabI	MLAAEAVTPIRR	Cys-210	6.69	4.41	63.19	2.88	56.50	1.1E-04	8558	6.5	5	enoyl-acyl-carrier-protein reductase, NADH-dependent
govT	ALVFEAGVKPCGLGAR	Cys-219	6.60	4.44	75.48	3.43	69.88	4.7E-05	3606	26.4	4	aminomethyltransferase, subunit (1 protein) of glycine cleavage complex
gpdD	GLSLVLEADQDLACATSSASSK	Cys-39	6.28	3.32	47.59	3.64	41.30	2.9E-04	11178	32.1	6	s-glycyl-3-phosphate dehydrogenase, aerobic, FAD/NAD(P)-binding
gpkK	NTYGTGCFMLMNTGK	Cys-270	8.15	4.00	64.13	1.62	55.95	3.7E-04	32476	3.3	6	glycerol kinase
	RTAIECHLKR	Cys-113	9.46	4.89	62.31	2.27	52.85	1.6E-04	32476	2.6	6	
	GGTRFSPAGDQDQAAFGQLCVK	Cys-256	8.53	4.15	53.51	0.66	44.98	1.1E-04	32476	6.1	7	
gPIA	GVFTDFPFFSTASCEK	Cys-53	4.49	0.93	71.96	3.72	66.57	6.5E-04	13800	6.4	5	citrate synthase
gPIB	SRESASGNTGCVYATGGR	Cys-1329	0.00	0.00	58.37	3.39	58.37	9.4E-03	6	5.9	9	glutamate synthase, large subunit
gnd	IAVAEDGEPCTVIGADGAGHYVK	Cys-169	7.43	4.62	61.68	2.18	54.25	1.1E-04	15285	18.9	9	6-phosphogluconate dehydrogenase, decarboxylating
gnd	FICQTDHSHLEQK	Cys-83	11.91	4.83	76.65	1.32	64.74	7.8E-04	2850	24.1	7	glycine C-acetyltransferase
gnd	VLAGDSVGVYDDESSCYPLTTIKQDFR	Cys-281	8.33	4.65	42.92	9.15	34.59	8.9E-03	0	24.9	3	lactose-inducible lac operon transcriptional repressor
gnd	VCLGTPLEK	Cys-45	6.48	3.59	57.52	1.23	51.04	7.4E-04	2415	2.7	7	luciferase
gnd	ALQEGQVCEAVGEGDQYAR	Cys-251	4.18	3.28	62.76	4.16	58.58	6.9E-05	86228	10.5	4	malate dehydrogenase, NAD(P)-binding
nanA	UAHVGVCSVAESQOOLAASK	Cys-82	7.32	4.42	86.44	19.17	79.13	4.7E-03	11291	7.3	6	N-acetylureamylase
nanF	ALHREGGQPSDEITELQCLR	Cys-388	31.27	12.61	89.34	8.14	58.07	6.4E-03	2031	5.3	2	NADH:ubiquinone oxidoreductase, chain F
pgk	LLTTGPNPSPDVR	Cys-289	7.72	4.25	63.57	3.93	55.67	6.5E-04	41675	5.8	7	phosphoglycerate kinase
	RLLTTCNIPVSPDVR	Cys-249	7.97	4.11	65.55	2.85	57.58	9.0E-05	41675	5.8	7	
pykA	VCLGAEKPSVSVK	Cys-338	7.65	4.73	60.19	2.23	52.55	1.4E-04	2359	2	7	pyruvate kinase II
sdhA	GSYVVDQDAEYMK	Cys-89	1.88	2.66	96.36	12.35	84.47	7.0E-04	6617	2.6	4	succinate dehydrogenase, flavoprotein subunit
sdhB	NGLALFRIDNIGPQK	Cys-75	25.42	10.96	85.38	0.67	61.96	1.4E-03	92989	2.4	8	succinate dehydrogenase, Fe/S subunit
sdhC	YGLPAPVGYCTPIR	Cys-265	10.36	4.89	75.83	4.66	65.47	1.5E-04	18969	3.6	9	succinyl-CoA synthetase, beta subunit
sdhD	WCGDFTSQDGFHSEQAIVGTYK	Cys-13	9.79	3.79	61.58	4.13	51.78	2.0E-04	21676	1.5	6	succinyl-CoA synthetase, NAD(P)-binding, alpha subunit
tdkA	AVTDKPSLMCK	Cys-243	8.50	4.87	69.16	1.18	60.66	1.0E-03	5321	2.5	5	transketolase 1, thiamine triphosphate-binding
ucaC	TLYVCLNPK	Cys-350	4.13	4.02	53.54	6.75	49.41	8.8E-04	166	4.6	8	uracil isomerase
Nucleotide metabolism												
deoB	IAFYANGCTIK	Cys-267	9.94	7.02	81.23	13.29	71.29	2.6E-03	9560	49.6	4	phosphonotomase
	IAFYANGCTIK	Cys-267	9.29	6.25	70.71	1.74	61.41	1.8E-04	9560	49.6	4	
guaB	VIGPISGICITTR	Cys-305	9.38	7.09	73.58	4.25	64.20	3.9E-04	3974	5.9	9	IMP dehydrogenase
ndk	EIAYFFGEGEVCPR	Cys-139	9.90	4.70	66.52	2.89	56.61	1.3E-04	15546	27.2	7	multifunctional nucleoside diphosphate kinase
pyrI	YCBKFSHNVLAN	Cys-141	16.57	5.77	87.71	8.70	71.14	6.5E-04	349	16	9	aspartate carbamoyltransferase, regulatory subunit
topA	CGTAMSDYLDPKR	Cys-665	6.85	9.69	100.00	0.00	93.15	2.7E-03	602	28.4	2	DNA topoisomerase I, omega subunit
Transport												
galP	VNIEYMDGVHLICTAK	Cys-55	1.88	2.66	65.08	3.97	63.20	6.2E-05	12599	1.9	7	galactitol-specific enzyme IIB component of PTS
ptsI	AVAEAGSSQAVVR	Cys-324	11.15	4.89	72.27	8.56	61.12	9.3E-04	5143	6.6	6	PEP:protein phosphotransferase of PTS system (enzyme I)
Protein metabolism												
aspC	CTOELLFGK	Cys-77	7.16	2.81	68.64	4.81	61.69	1.9E-04	3586	16.6	3	aspartate aminotransferase, PLP-dependent
	CTOELLFGK	Cys-77	7.10	3.43	51.04	4.17	43.94	3.3E-04	3586	16.6	3	
	FAADHFVYSR	Cys-397	11.05	9.85	83.02	13.18	71.97	3.5E-03	130	2.2	3	succinylornithine transaminase, PLP-dependent
lysA	ALDGGPFGKALLETAEK	Cys-250	5.30	2.58	58.58	7.23	53.58	1.5E-04	130	5	3	protein chain elongation factor EF-G, GTP-binding
	AAADIAAGLKVDTGCTDLPDAPILER	Cys-398	5.49	6.24	100.00	0.00	94.51	1.1E-03	66528	17.8	5	
	VLNNEILVTCGSAPK	Cys-266	2.95	2.70	69.65	4.35	66.69	8.8E-05	66528	20.2	3	
ivcC	KVVVVGCGAQLNGLNMR	Cys-45	10.45	4.58	75.89	17.15	65.44	6.5E-03	1148	6.1	9	ketol-acid reductoisomerase, NAD(P)-binding
ribB	FGAAGCVTGESVVKR	Cys-815	7.89	4.44	43.01	2.48	35.12	6.2E-04	3236	2.5	7	translation initiation factor IF-2
ribC	FALEKAEKAVDLVEISPAEPCVCR	Cys-65	3.69	3.27	84.48	8.14	40.40	2.9E-03	17047	3	7	translation initiation factor IF-3
rne	CSGTVTRDNESSLISLR	Cys-407	23.53	6.08	93.02	9.88	69.48	1.1E-03	1150	9.4	9	endoribonuclease; RNA-binding protein; RNA degradome binding protein
rpmE	IRTVGDLHDLVCSK	Cys-37	25.16	7.59	89.15	2.80	63.98	3.6E-04	44769	12.7	9	50S ribosomal subunit protein L31
rpmE	STFVGDHDLVDVCSK	Cys-37	26.07	8.35	86.53	5.00	60.45	9.3E-04	44769	12.7	9	
rpmE	LLYVDVGVYR	Cys-44	9.52	4.76	1.40	2.40	10.88	9.4E-03	160.8	16.8	4	RNA polymerase, alpha subunit
rpmB	LGEPVDFVQECIR	Cys-85	3.33	2.37	77.03	16.57	73.70	3.4E-03	5649	2.7	8	RNA polymerase, beta subunit
rpmB	ISLGLKQCK	Cys-349	8.13	4.66	66.12	5.88	57.99	4.0E-04	46364	3.3	3	30S ribosomal subunit protein S1

¹⁶Schmidt, A., Kochanowski, K., Vedraar, S., Ahn, E., Volkmer, B., Callipo, L., Knopp, K., Bauer, M., Aebbers, R., and Heinemann, M. (2016). The quantitative and condition-dependent Escherichia coli proteome. Nat. Biotechnol. 34, 104-110.

Fig. 7. Relative oxidation of OxICAT identified redox-active cysteine of *E. coli* having encountered neutrophil phagocytosis with a difference of > 30% thiol-oxidation after phagocytosis when compared to extracellular bacteria and $p < 0.01$. Intracellular *E. coli* cells (Treated) were separated from extracellular bacteria (Control) and enriched according to Fig. 1E. The relative cysteine oxidation was determined using OxICAT. The average changes of thiol-oxidation after neutrophil phagocytosis (Δ Cys-Oxidation) was determined by the difference between the treated (\emptyset Treated) and the control (\emptyset Control) samples. Protein function according to UniProt. The protein abundance was obtained from a protein expression database from *E. coli* MG1655 growing in LB medium (a)Schmidt et al. 2016). The relative surface accessibility of identified cysteines was calculated using NetSurfP and the cysteine-conservation determined using ConSurf. Values generated from three independent experiments.

Gene	Sequence	Identified Cysteine	Ø Control Cys-Oxidation [%]	Control SD [%]	Ø Treated Cys-Oxidation [%]	Treated SD [%]	ΔCys-Oxidation ØTreated-ØControl [%]	p-value t-test	Average ^{cell} copies/cell	Surface accessibility of identified cysteine [%]	Cys-conservation (1-9)	Description
Protein metabolism (continued)												
rpmB	DAALSCDDFFVNHK	Cys-87	5.99	2.77	67.18	11.51	61.19	1.8E-03	89526	5.2	4	30S ribosomal subunit protein S2
rpmS	SNVPALEACPQKR	Cys-27	12.14	5.44	74.33	4.45	62.19	2.3E-04	6947	16.2	1	30S ribosomal subunit protein S12
rpmL	LMKLGCVYR	Cys-85	7.33	3.34	53.53	1.78	46.21	1.9E-04	87952	17.1	5	30S ribosomal subunit protein S13
rpmL	LHVHNVKNECGDQWVEIR	Cys-63	13.91	6.30	53.17	0.59	43.26	3.9E-04	17289	8.7	4	30S ribosomal subunit protein S17
rpmU	TTKLHVHNNENCGDQWVEIR	Cys-53	13.58	6.48	60.49	1.49	46.90	5.7E-04	17289	8.7	4	
rspA	SCBEKAVLAEVR	Cys-23	9.76	3.22	54.65	8.85	44.89	2.5E-03	8339	5.6	5	30S ribosomal subunit protein S21
tgt	ILEHVCPQIPADKPR	Cys-232	5.79	4.66	74.00	4.32	68.20	1.1E-04	847	22.8	1	tRNA-guanine transglycosylase
trfS	RVPFVMPVGDVEVSKK	Cys-596	4.68	3.34	75.83	17.13	71.14	4.5E-03	1256	2.4	6	threonyl-tRNA synthetase
tsaA	DDSPFDYITPCR	Cys-294	8.59	7.04	86.81	2.48	78.23	1.2E-04	138625	4.7	2	tryptophan-L-cysteine desulfurylase, PLP-dependent
	LLPHIPADQFAQALACELYK	Cys-383	3.89	3.86	81.80	2.72	77.92	2.4E-05	138625	10.5	4	
	LVVVOEGFPFTYGGLEGAMER	Cys-298	8.89	4.67	75.00	8.66	66.11	6.8E-04	138625	31.6	6	
	MVAFVSNVYFDTTQGHSGINGQVTR	Cys-148	5.30	2.25	46.30	5.90	40.99	7.8E-04	138625	7.9	6	
trpC	RLLGKNSGCLTR	Cys-261	10.55	5.41	76.71	16.90	66.17	6.5E-03	46	19.6	9	indole-3-glycerol phosphate synthetase
	VLLGENKVGSLTR	Cys-261	10.42	4.91	67.96	11.76	57.53	3.1E-03	46	19.6	9	
	TAFLECK	Cys-55	6.08	2.26	40.46	3.92	34.88	4.3E-04	46	6.2	9	
tufB	HYAHVDCPHADYVK	Cys-82	8.32	4.59	72.01	9.57	63.69	1.1E-03	0	5.4	7	translation elongation factor EF-Tu 2
Detoxification & Stress response												
groL	AVTAAVEELKALVPCSDSK	Cys-138	1.14	0.88	61.43	8.25	60.29	5.0E-04	85698	16.2	6	Cpn60 chaperonin GroEL, large subunit of GroESL
icd	LLKSEFGDAEIMK	Cys-405	6.48	3.48	49.64	9.18	43.16	3.4E-03				

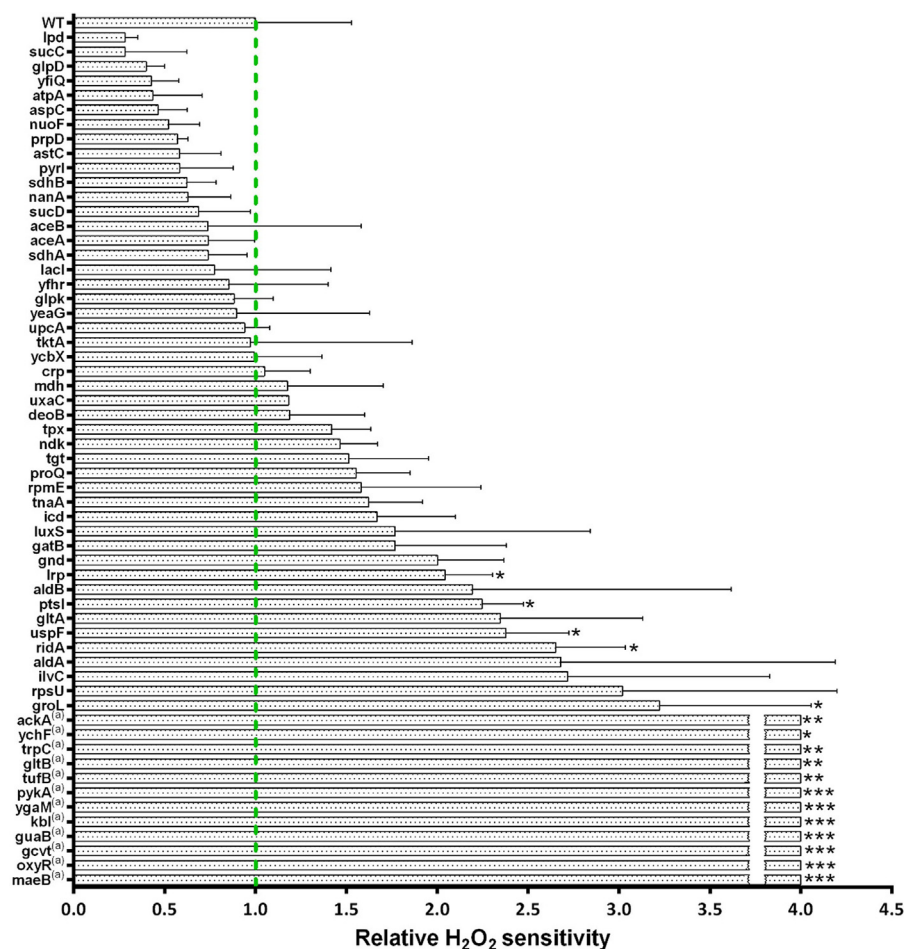


Fig. 9. H₂O₂ sensitivity of 59 *E. coli* deletion strains. *E. coli* wild type as well as 59 deletion strains chosen based on the OxICAT analysis were grown in LB medium at 37 °C. Mid-logarithmic cultures were split and grown in the absence and presence of 2.5 mM H₂O₂ in LB medium for 13.5 h. *E. coli* wild type needed approximately 5 h until it reached an OD₆₀₀ = 0.2 in H₂O₂-containing media (see Fig. 8). The time needed for individual strains to reach an OD₆₀₀ = 0.2 was used to calculate their relative H₂O₂ sensitivity in comparison to wild type. For a description of the calculation see part “Hydrogen peroxide growth inhibition assay” of the Materials and Methods section. Strains, that did not reach OD₆₀₀ = 0.2 over 13.5 h were assigned the relative sensitivity value 4. All strains were normalized to the growth of WT *E. coli* cells (green dotted line). Significant difference compared to the WT cells was determined using Student’s *t*-test (*: 0.01 < *p* < 0.05, **: 0.001 < *p* < 0.01, ***: *p* < 0.001). Error bars show standard deviation.

could be covered. In a quantitative condition-dependent *E. coli* proteome study, Schmidt et. al identified and quantified 2019 proteins from *E. coli* MG1655 grown in LB [54]. Thus, we cover only around 5.7% of the proteins that are known to be expressed in *E. coli* MG1655. The presence of contaminating host protein is probably, at least in part, reason for our limited coverage of *E. coli*'s proteome, and has been found to occur in other proteomic studies of bacteria-host interactions [70]. Additionally, the reactive group iodoacetamide of the ICAT reagent only reacts with reversibly oxidized thiols. It has been estimated that 5% of cellular protein cysteines are oxidized to sulfenic acids, an irreversibly oxidized form of thiol that does not react with iodoacetamide and could not be identified in the LC-MS analysis [25].

In the control fraction, the vast majority, 135 peptides (78.0%) showed a thiol oxidation level of less than 20%, including 105 cysteine peptides (60.7%) with an oxidized fraction below 10% (Fig. 4). This indicates that most of the identified cysteine thiols were in their reduced state, suggesting that the cytoplasm of *E. coli* outside of the neutrophils is in an overall reducing state, as exemplified by the cytoplasmic glutamate synthase protein GltB (Fig. 5C). 23 peptides (12.7%) showed an oxidation level higher than 60% (Figs. 3 and 4 and Supplementary Table 1). These highly thiol-oxidized proteins include periplasmic and outer membrane proteins such as OmpA (outer membrane protein A, up to 99.6% oxidized) and DppA (heme ABC transporter, up to 88.1% oxidized), which are known to harbor oxidized cysteine in the form of structural disulfide bonds and have already been reported as basal-level thiol-oxidized in *E. coli* (Fig. 5A) [37]. The resolving cysteine Cys-166 of AhpC (alkyl hydroperoxide reductase) was oxidized 78.6% in the control fraction containing extracellular *E. coli* (we were not able to identify the peptide containing the peroxidatic cysteine of AhpC in our experiments). This oxidation was more than

40% higher than the oxidized fraction of the resolving cysteine of AhpC we observed in *E. coli* cultured in minimal medium [37]. This increase in basal-level oxidation of this hydroperoxide detoxifying enzyme suggests that *E. coli* in close proximity to neutrophils already encounter a low-level of oxidative stress through oxidants such as H₂O₂ and monochloramine. These oxidants are produced in the phagosome and have been shown to be membrane permeable [23,68].

In contrast to the overall low oxidation state of thiols in extracellular bacteria, *E. coli* that directly encountered neutrophil phagocytosis showed a thiol oxidation level of higher than 30% in 162 peptides (93.7%). These included 118 peptide cysteines (68.2%) oxidized even more than 60% (Figs. 3 and 4 and Supplementary Table 1). Thus, the majority of identified cysteine residues in phagocytized bacteria were in an oxidized state.

3.2. Thiol-oxidized proteins from phagocytized *E. coli* are involved in protein and carbon metabolism

To identify protein thiols that were affected by neutrophil phagocytosis, we compared the relative thiol oxidation state of phagocytized bacteria with that of extracellular bacteria. To select a set of significantly more oxidized cysteines in the phagocytized *E. coli*, Student's *t*-tests were performed on the identified 173 cysteine-containing peptides. For the *t*-test, the percentage mean values of heavy-ICAT-labeled cysteine from each peptide were compared. Based on the mean values, significance in cysteine oxidation was determined between extracellular and phagocytized *E. coli*. The difference in thiol oxidation between those two samples as well as their respective *p*-values were then graphed onto a volcano plot. As thresholds, cysteine oxidation difference was set to 30% (non-axial vertical line) and the respective *p*-value

to 0.01 (non-axial horizontal line). In this way, 102 peptide-containing cysteines representing 76 proteins were binned and showed a highly significant increase in thiol oxidation of more than 30% (Figs. 6A and 7, Supplementary Table 2). The identified significantly oxidized proteins were predominantly from major metabolic pathways (Fig. 6B, C). In agreement with proteomic studies done with intracellular *Salmonella* species, most of the identified proteins were related to housekeeping functions [3,59]. However, based on the *E. coli* genome, a noticeable high proportion of the identified proteins (16%) were involved in stress response and detoxification.

27% of the identified proteins were involved in protein synthesis. Amongst those, a significant number were ribosome associated proteins including Rne (ribonuclease E) and RpmE (50 S ribosomal protein L31), both showed oxidation at their conserved Zn-binding CXXC-motif. Further, essential components for the initiation of protein synthesis, including the translation initiation factors InfB (Cys-815) and InfC (Cys-65) were thiol-oxidized. Both RpmE and InfC have been shown to be oxidized in *E. coli* after HOCl-treatment [37]. Other oxidized proteins include FusA (elongation factor G), RpoA (DNA-directed RNA polymerase subunit alpha), RpsL (30S ribosomal protein S12) and RpsM (30S ribosomal protein S13). These were reported to be thiol-oxidized after allicin treatment, a thiol-oxidizing component from garlic that induces the oxidative and heat stress response in *E. coli* [47]. In addition, RpsM was identified as conserved S-thiolated protein in different Gram-positive bacteria under HOCl stress, such as *Corynebacterium glutamicum* and *Mycobacterium smegmatis* [7,29]. The queuine tRNA-ribosyltransferase Tgt showed also increased oxidations under HOCl stress in *Staphylococcus aureus* [31]. The ketol-acid reductoisomerase IlvC, which was modified at the conserved Cys-45 after phagocytosis, is involved in the biosynthesis of isoleucine and valine. IlvC has been shown to harbor cysteine residues that were modified in *E. coli* under nitrosative stress, however the cysteines affected by NO• were not determined in that study [5]. In addition, TrpC (tryptophan biosynthesis protein TrpCF) was oxidized at Cys-261 and Cys-55. The significant amounts of identified proteins involved in translation and transcription suggests an inhibition of protein synthesis upon phagocytosis. Previous studies have shown that treatment with oxidants leads to the inhibition of protein synthesis in bacteria [19,20,40,57]. Inhibition of protein synthesis upon phagocytosis might be used by host immune cells to stop cell division in bacteria. However, it has also been shown, that inhibition and reprogramming of transcription is used by bacteria to protect themselves against oxidative stress. Thus, it is possible that the inhibition of protein synthesis might be used initially by *E. coli* to respond to increased oxidative stress during the formation of the phagosome [19,40].

44% of all significantly oxidized proteins were from either carbohydrate or nucleotide metabolism. Oxidized conserved thiols were found in AceA (isocitrate lyase, Cys-195), Gnd (6-phosphogluconate dehydrogenase, Cys-169), AtpA (ATP synthase subunit alpha, Cys-193), GuaB (IMP dehydrogenase, Cys-305), PyrI (aspartate transcarbamoylase, Cys-141) and SdhB (membrane-bound succinate dehydrogenase, Cys-75). Both AceA and GuaB were oxidized at their respective active site cysteines and hence most likely inactivated in phagocytized *E. coli*. GuaB belongs to the most conserved S-thiolated proteins in different Gram-positive bacteria [31]. AceA is used by *E. coli* to bypass the TCA cycle and enables the use of carbon substrates at the level of acetyl-CoA including fatty acids and alcohols [42]. AceA has been previously shown to be S-mycothiolated in *M. smegmatis* upon HOCl-treatment [29]. SdhB and the regulatory chain of PyrI were oxidized at their respective metal-binding sites. In addition to the implied inhibition of protein synthesis, we observed that neutrophil phagocytosis leads to the oxidation of proteins involved in major metabolic pathways and thus potentially their inactivation.

3.3. Neutrophil phagocytosis leads to thiol oxidation of antioxidant proteins and proteins involved in cell detoxification

Amongst the proteins in *E. coli* that were significantly thiol-oxidized after phagocytosis, some were known to be involved in the oxidative and heat shock stress response including Tpx (thiol peroxidase), RidA (enamine/imine deaminase), GroL (60 kDa chaperonin), ProQ (RNA chaperone) and OxyR (hydrogen peroxide-inducible genes activator). Tpx, a highly conserved thiol-specific peroxidase that preferentially catalyzes the reduction of alkyl hydroperoxides [24] was oxidized at both the peroxidatic cysteine (Cys-61) and the resolving cysteine (Cys-95) (Fig. 7, Supplementary Table 2). Tpx from different species were found more thiol-oxidized under HOCl-stress, including Tpx from *E. coli*, *M. smegmatis* and *S. aureus* [29,31,37]. RidA, that functions as a chaperone once N-chlorinated [46], was found 40% more oxidized at its conserved cysteine C107 after phagocytosis. Although the chaperone activity has been reported to be independent of C107, oxidation of this cysteine has been reported previously after peroxynitrite and allicin stress [39,46,47]. Other thiol-oxidized chaperones include GroL and ProQ. GroL promotes protein refolding under stress conditions and is known to be heat-responsive in *E. coli* [9]. Interestingly, GroL of the closely related *S. Typhimurium* was found induced during infection of macrophages [6]. ProQ was found to be involved in the DNA-damage response [61]. This points towards the possibility that both *E. coli* proteins involved in DNA-damage and protein-damage response are functionally occupied due to the oxidative environment present in the phagolysosome.

C259 from OxyR was also found oxidized (65.7%) after phagocytosis (Fig. 5E, F). OxyR is a master-regulator that controls the expression of antioxidant genes in response to both oxidative and nitrosative stress [26,63,71]. This is underlined by hypersensitivity of *oxyR* deletion mutants to hydrogen peroxide treatment and increased frequency of spontaneous mutagenesis [22,63]. Redox signaling through OxyR is typically mediated by a disulfide formation between C199 and C208 [71]. Although we couldn't identify peptides from OxyR containing either of the two cysteines, it has been shown that C259 forms a disulfide bond with C180. It was suggested that this disulfide bond might influence the regulatory mechanism of OxyR by facilitating disulfide formation of C199 and C208 [35].

3.4. Proteins modified upon neutrophil phagocytosis are needed by *E. coli* to overcome oxidative stress

One important weapon in the arsenal of a professional phagocytic cell is the production of different oxidative species. While HOCl is probably the most effective thiol oxidant released in the phagolysosome [14], other oxidants, such as hydrogen peroxide, are also present in high abundance and can lead to the damage of bacterial structures. To identify proteins with a potential antioxidant effect in *E. coli* during phagocytosis, we treated exponentially growing deletion strains with 2.5 mM H₂O₂ and measured the subsequent growth for 810 min (Fig. 8). From the 76 proteins significantly oxidized during phagocytosis, 17 were essential for *E. coli*. Thus, 59 deletion mutants lacking the non-essential genes were tested for H₂O₂-sensitivity. Several strains tested seemingly showed a lower relative H₂O₂ sensitivity (Fig. 9), however the differences were not significant and these strains typically already showed a growth defect under non-stress conditions (Fig. 8). On the other hand, 16 mutant strains showed significantly compromised growth upon treatment with H₂O₂ when compared to wild type (Figs. 8 and 9). Amongst those, 11 strains did not reach an OD₆₀₀ of 0.2 during the duration of our measurement (810 min). Thus, the respective genes deleted in these 11 mutants are essential for efficient growth of *E. coli* in the presence of H₂O₂ (Fig. 9).

Similar to previous studies, the quorum-sensing mutants $\Delta luxS$ and $\Delta traA$ were not sensitive to H₂O₂ [36]. However, an *E. coli* mutant lacking the leucine-responsive regulatory protein Lrp has been shown to

be more resistant to hydroperoxide stress [13]. In addition, over-expression of YchF, a highly conserved ATPase was shown to lead to H₂O₂ hypersensitivity in *E. coli* [66]. In agreement with previous studies, mutants lacking proteins that are important for the oxidative stress response, such as OxyR and RidA were significantly growth compromised [33,46]. Furthermore, the heat shock responsive chaperone GroL, the malate dehydrogenase MaeB and the general stress responsive protein UspF were shown to be important for the growth of *E. coli* exposed to H₂O₂-stress [9,48]. Similar to *Listeria monocytogenes*, the glutamate synthase GltB was shown in this study to be important for *E. coli* to respond to oxidative stress [30]. The hydrogen peroxide hypersensitivity of a *maeB* deletion mutant was reported for *S. Typhimurium*, and its sensitivity towards peroxyxynitrite was shown in *E. coli* [28,38]. Both GltB and MaeB share the ability to reduce NADP⁺ to NADPH. NADPH is crucial for the functionality of cellular antioxidant enzymes including glutathione reductase and thioredoxin reductase [10,11]. In addition, as suggested by Henard et. al, reduced generation of pyruvate (an effective scavenger of oxidants) might lead to the increased hydrogen peroxide sensitivity of a *maeB* deletion mutant [28,49].

Some growth-inhibited mutants have not been reported to be responsive to oxidative stress. These include the metabolic enzymes TrpC (tryptophan biosynthesis protein) and Kbl (glycine C-acetyltransferase). Combined with our findings from the OxICAT analysis, our study highlighted the essentiality of some of those metabolic enzymes for the survival of *E. coli* under oxidative stress.

4. Conclusion

In humans, neutrophils are the most abundant circulating leukocytes. They are immediately recruited to sites of inflammation to eliminate invading pathogens. Pathogens, such as bacteria, are then engulfed and trapped in phagosomes once they encounter neutrophils. In the phagosomes, bacteria are attacked by a complex mixture of different oxidants produced by the neutrophils. We studied the effects of neutrophil phagocytosis on the thiol proteome of bacteria. Based on our data, we conclude that neutrophil phagocytosis leads to an overall break-down of the *E. coli* protein thiol homeostasis. Amongst the proteins we identified were numerous proteins needed by *E. coli* to survive oxidative stress. Thus, our study suggests that a systemic oxidation of protein thiols might be a general antimicrobial mechanism that neutrophils have at their disposal to counteract invading bacteria.

CRedit authorship contribution statement

Kaibo Xie: Conceptualization, Data curation, Formal analysis, Investigation, Methodology, Validation, Visualization, Writing - original draft. **Christina Bunse:** Data curation, Investigation, Methodology. **Katrin Marcus:** Funding acquisition, Resources, Writing - review & editing. **Lars I. Leichert:** Conceptualization, Data curation, Funding acquisition, Methodology, Project administration, Writing - original draft, Writing - review & editing.

Acknowledgments

Principal funding was provided by the German Research Foundation (DFG) through grant LE2905/1-2 to LIL as part of the priority program 1710 'Dynamics of Thiol-based Redox Switches in Cellular Physiology'. Parts of this manuscript were written during a Writing Retreat funded by the Ruhr-Universität Bochum Research School RURS^{plus}.

Appendix A. Supporting information

Supplementary data associated with this article can be found in the online version at doi:10.1016/j.redox.2018.101087

References

- [1] H. Ashkenazy, S. Abadi, E. Martz, O. Chay, I. Mayrose, T. Pupko, N. Ben-Tal, ConSurf 2016: an improved methodology to estimate and visualize evolutionary conservation in macromolecules, *Nucleic Acids Res.* 44 (2016) W344–W350.
- [2] T. Baba, T. Ara, M. Hasegawa, Y. Takai, Y. Okumura, M. Baba, K.A. Datsenko, M. Tomita, B.L. Wanner, H. Mori, Construction of *Escherichia coli* K-12 in-frame, single-gene knockout mutants: the Keio collection, *Mol. Syst. Biol.* 2 (2006) 2006.0008.
- [3] D. Becker, M. Selbach, C. Rollenhagen, M. Ballmaier, T.F. Meyer, M. Mann, D. Bumann, Robust *Salmonella* metabolism limits possibilities for new antimicrobials, *Nature* 440 (2006) 303–307.
- [4] G.M. Bokoch, B. Diebold, J.-S. Kim, D. Gianni, Emerging Evidence for the Importance of Phosphorylation in the Regulation of NADPH Oxidases, *Antioxid. Redox Signal.* 11 (2009) 2429–2441.
- [5] N. Brandes, A. Rinck, L.I. Leichert, U. Jakob, Nitrosative stress treatment of *E. coli* targets distinct set of thiol-containing proteins, *Mol. Microbiol.* 66 (2007) 901–914.
- [6] N.A. Buchmeier, F. Heffron, Induction of *Salmonella* stress proteins upon infection of macrophages, *Science* 248 (1990) 730–732.
- [7] T. Busche, R. Silar, M. Pičmanová, M. Pátek, J. Kalinowski, Transcriptional regulation of the operon encoding stress-responsive ECF sigma factor SigH and its anti-sigma factor RshA, and control of its regulatory network in *Corynebacterium glutamicum*, *BMC Genom.* 13 (2012) 445.
- [8] S.M. Chiang, H.E. Schellhorn, Regulators of oxidative stress response genes in *Escherichia coli* and their functional conservation in bacteria, *Arch. Biochem. Biophys.* 525 (2012) 161–169.
- [9] S.E. Chuang, F.R. Blattner, Characterization of twenty-six new heat shock genes of *Escherichia coli*, *J. Bacteriol.* 175 (1993) 5242–5252.
- [10] J.-F. Collet, J. Messens, Structure, function, and mechanism of thioredoxin proteins, *Antioxid. Redox Signal.* 13 (2010) 1205–1216.
- [11] N. Couto, J. Wood, J. Barber, The role of glutathione reductase and related enzymes on cellular redox homeostasis network, *Free Radic. Biol. Med.* 95 (2016) 27–42.
- [12] J. Cox, M. Mann, MaxQuant enables high peptide identification rates, individualized p.p.b.-range mass accuracies and proteome-wide protein quantification, *Nat. Biotechnol.* 26 (2008) 1367–1372 (PubMed PMID: 19029910).
- [13] P. De Spiegeleer, K. Vanoirbeek, A. Lietaert, J. Sermon, A. Aertsen, C.W. Michiels, Investigation into the resistance of lactoperoxidase tolerant *Escherichia coli* mutants to different forms of oxidative stress, *FEMS Microbiol. Lett.* 252 (2005) 315–319.
- [14] A. Degrossoli, A. Müller, K. Xie, J.F. Schneider, V. Bader, K.F. Winkhofer, A.J. Meyer, L.I. Leichert, Neutrophil-generated HOCl leads to non-specific thiol oxidation in phagocytized bacteria, *eLife* 7 (2018) e32288.
- [15] F.R. DeLeo, L.-A.H. Allen, M. Apicella, W.M. Nauseef, NADPH oxidase activation and assembly during phagocytosis, *J. Immunol.* 163 (1999) 6732–6740.
- [16] S.R. Eddy, Accelerated profile HMM searches, *PLoS Comput. Biol.* 7 (2011) e1002195.
- [17] A. El Chemaly, Y. Okochi, M. Sasaki, S. Arnaudeau, Y. Okamura, N. Demareux, VSOP/Hv1 proton channels sustain calcium entry, neutrophil migration, and superoxide production by limiting cell depolarization and acidification, *J. Exp. Med.* 207 (2010) 129–139.
- [18] M. Ellison, G. Thurman, D.R. Ambruso, Myeloid cells differentiated in the presence of interferon- γ (inf- γ) compared to mature cells exposed to this cytokine exhibit different phox protein expression and Nox2 activity, *Blood* 124 (2014) (4103–4103).
- [19] Y. Fan, J. Wu, M.H. Ung, N. De Lay, C. Cheng, J. Ling, Protein mistranslation protects bacteria against oxidative stress, *Nucleic Acids Res.* 43 (2015) 1740–1748.
- [20] C.M. Grant, Regulation of translation by hydrogen peroxide, *Antioxid. Redox Signal.* 15 (2011) 191–203.
- [21] M.J. Gray, Y. Li, L.I. Leichert, Z. Xu, U. Jakob, Does the transcription factor NemR use a regulatory sulfenamide bond to sense bleach? *Antioxid. Redox Signal.* 23 (2015) 747–754 (PMID: 25867078).
- [22] J.T. Greenberg, B. Demple, Overproduction of peroxide-scavenging enzymes in *Escherichia coli* suppresses spontaneous mutagenesis and sensitivity to redox-cycling agents in oxyR-mutants, *EMBO J.* 7 (1988) 2611–2617.
- [23] M.B. Grisham, M.M. Jefferson, D.F. Melton, E.L. Thomas, Chlorination of endogenous amines by isolated neutrophils. ammonia-dependent bactericidal, cytotoxic, and cytolytic activities of the chloramines, *J. Biol. Chem.* 259 (1984) 10404–10413.
- [24] A. Hall, B. Sankaran, L.B. Poole, P.A. Karplus, Structural changes common to catalysis in the Tpx peroxiredoxin subfamily, *J. Mol. Biol.* 393 (2009) 867–881.
- [25] M. Hamann, T. Zhang, S. Hendrich, J.A. Thomas, Quantitation of protein sulfenic and sulfonic acid, irreversibly oxidized protein cysteine sites in cellular proteins, in: H. Sies, L. Packer (Eds.), *Methods in Enzymology*, Academic Press, 2002, pp. 146–156.
- [26] A. Hausladen, C.T. Privalle, T. Keng, J. DeAngelo, J.S. Stamler, Nitrosative stress: activation of the transcription factor OxyR, *Cell* 86 (1996) 719–729.
- [27] J. Heijden, E.S. van der, Bosman, L.A. Reynolds, B.B. Finlay, Direct measurement of oxidative and nitrosative stress dynamics in *Salmonella* inside macrophages, *Proc. Natl. Acad. Sci.* 112 (2015) 560–565.
- [28] C.A. Henard, T.J. Bourret, M. Song, A. Vázquez-Torres, Control of redox balance by the stringent response regulatory protein promotes antioxidant defenses of *Salmonella*, *J. Biol. Chem.* 285 (2010) 36785–36793.
- [29] M. Hillion, J. Bernhardt, T. Busche, M. Rossius, S. Maaß, D. Becher, M. Rawat, M. Wirtz, R. Hell, C. Rückert, et al., Monitoring global protein thiol-oxidation and protein S-mycylation in *Mycobacterium smegmatis* under hypochlorite stress, *Sci. Rep.* 7 (2017) 1195.

- [30] Y. Huang, Y. Suo, C. Shi, J. Szlavik, X.-M. Shi, S. Knöchel, Mutations in gltB and gltC reduce oxidative stress tolerance and biofilm formation in *Listeria monocytogenes* 4b G, *Int. J. Food Microbiol.* 163 (2013) 223–230.
- [31] M. Imber, A.J. Pietrzyk-Brzezinska, H. Antelmann, Redox regulation by reversible protein S-thiolation in Gram-positive bacteria, *Redox Biol.* 20 (2018) 130–145.
- [32] U. Jakob, W. Muse, M. Eser, J.C.A. Bardwell, Chaperone activity with a redox switch, *Cell* 96 (1999) 341–352.
- [33] J.R. Johnson, C. Clabots, H. Rosen, Effect of inactivation of the global oxidative stress regulator *oxyR* on the colonization ability of *Escherichia coli* O1:K1:H7 in a mouse model of ascending urinary tract infection, *Infect. Immun.* 74 (2006) 461–468.
- [34] K. Katoh, D.M. Standley, MAFFT multiple sequence alignment software version 7: improvements in performance and usability, *Mol. Biol. Evol.* 30 (2013) 772–780.
- [35] S.O. Kim, K. Merchant, R. Nudelman, W.F. Beyer, T. Keng, J. DeAngelo, A. Hausladen, J.S. Stamler, OxyR: a molecular code for redox-related signaling, *Cell* 109 (2002) 383–396.
- [36] J. Lee, S.R. Hiibel, K.F. Reardon, T.K. Wood, Identification of stress-related proteins in *Escherichia coli* using the pollutant cis-dichloroethylene, *J. Appl. Microbiol.* 108 (2010) 2088–2102.
- [37] L.I. Leichert, F. Gehrke, H.V. Gudiseva, T. Blackwell, M. Ilbert, A.K. Walker, J.R. Strahler, P.C. Andrews, U. Jakob, Quantifying changes in the thiol redox proteome upon oxidative stress in vivo, *Proc. Natl. Acad. Sci.* 105 (2008) 8197–8202.
- [38] C. Lindemann, L.I. Leichert, Quantitative redox proteomics: the NOxICAT method, *Methods Mol. Biol.* 893 (2012) 387–403.
- [39] C. Lindemann, N. Lupilova, A. Müller, B. Warscheid, H.E. Meyer, K. Kuhlmann, M. Eisenacher, L.I. Leichert, Redox proteomics uncovers peroxynitrite-sensitive proteins that help *Escherichia coli* to overcome nitrosative stress, *J. Biol. Chem.* 288 (2013) 19698–19714.
- [40] J. Ling, D. Söll, Severe oxidative stress induces protein mistranslation through impairment of an aminoacyl-tRNA synthetase editing site, *Proc. Natl. Acad. Sci.* 107 (2010) 4028–4033.
- [41] Y. Liu, Q. Zhang, M. Hu, K. Yu, J. Fu, F. Zhou, X. Liu, Proteomic analyses of intracellular *Salmonella enterica* serovar typhimurium reveal extensive bacterial adaptations to infected host epithelial cells, *Infect. Immun.* 83 (2015) 2897–2906.
- [42] S.R. Maloy, W.D. Nunn, Genetic regulation of the glyoxylate shunt in *Escherichia coli* K-12, *J. Bacteriol.* 149 (1982) 173–180.
- [43] L.S. Meena, null Rajni, Survival mechanisms of pathogenic *Mycobacterium tuberculosis* H37Rv, *FEBS J.* 277 (2010) 2416–2427.
- [44] R. Minakami, H. Sumimoto, Phagocytosis-coupled activation of the superoxide-producing phagocyte oxidase, a member of the NADPH oxidase (nox) family, *Int. J. Hematol.* 84 (2006) 193–198.
- [45] D.M. Monack, D.M. Bouley, S. Falkow, *Salmonella typhimurium* persists within macrophages in the mesenteric lymph nodes of chronically infected Nramp1 +/+ mice and can be reactivated by IFN γ neutralization, *J. Exp. Med.* 199 (2004) 231–241.
- [46] A. Müller, S. Langklotz, N. Lupilova, K. Kuhlmann, J.E. Bandow, L.I.O. Leichert, Activation of RidA chaperone function by N-chlorination, *Nat. Commun.* 5 (2014) 5804.
- [47] A. Müller, J. Eller, F. Albrecht, P. Prochnow, K. Kuhlmann, J.E. Bandow, A.J. Slusarenko, L.I.O. Leichert, Allicin induces thiol stress in bacteria through S-allylmercapto modification of protein cysteines, *J. Biol. Chem.* 291 (2016) 11477–11490.
- [48] L. Nachin, U. Nannmark, T. Nyström, Differential roles of the universal stress proteins of *Escherichia coli* in oxidative stress resistance, adhesion, and motility, *J. Bacteriol.* 187 (2005) 6265–6272.
- [49] J. O'Donnell-Tormey, C.F. Nathan, K. Lanks, C.J. DeBoer, J. de la Harpe, Secretion of pyruvate. An antioxidant defense of mammalian cells, *J. Exp. Med.* 165 (1987) 500–514.
- [50] B. Petersen, T.N. Petersen, P. Andersen, M. Nielsen, C. Lundegaard, A generic method for assignment of reliability scores applied to solvent accessibility predictions, *BMC Struct. Biol.* 9 (2009) 51.
- [51] C. Pivrot-Pajot, F.C. Chouinard, M.A. El Azreq, D. Harbour, S.G. Bourgoin, Characterisation of degranulation and phagocytic capacity of a human neutrophilic cellular model, PLB-985 cells, *Immunobiology* 215 (2010) 38–52.
- [52] L.B. Poole, The basics of thiols and cysteines in redox biology and chemistry, *Free Radic. Biol. Med.* 0 (2015) 148–157.
- [53] M.T. Quinn, K.A. Gauss, Structure and regulation of the neutrophil respiratory burst oxidase: comparison with nonphagocyte oxidases, *J. Leukoc. Biol.* 76 (2004) 760–781.
- [54] A. Schmidt, K. Kochanowski, S. Vedelaar, E. Ahrné, B. Volkmer, L. Callipo, K. Knoops, M. Bauer, R. Aebersold, M. Heinemann, The quantitative and condition-dependent *Escherichia coli* proteome, *Nat. Biotechnol.* 34 (2016) 104–110.
- [55] C.A. Schneider, W.S. Rasband, K.W. Eliceiri, NIH Image to ImageJ: 25 years of image analysis, *Nat. Methods* 9 (2012) 671–675 (PubMed PMID: 22930834).
- [56] A.W. Segal, The function of the NADPH oxidase of phagocytes and its relationship to other NOXs in plants, invertebrates, and mammals, *Int. J. Biochem. Cell Biol.* 40 (2008) 604–618.
- [57] D. Shenton, J.B. Smirnova, J.N. Selley, K. Carroll, S.J. Hubbard, G.D. Pavitt, M.P. Ashe, C.M. Grant, Global translational responses to oxidative stress impact upon multiple levels of protein synthesis, *J. Biol. Chem.* 281 (2006) 29011–29021.
- [58] V.L. Shepherd, The role of the respiratory burst of phagocytes in host defense, *Semin. Respir. Infect.* 1 (1986) 99–106.
- [59] L. Shi, J.N. Adkins, J.R. Coleman, A.A. Schepmoes, A. Dohnkova, H.M. Mottaz, A.D. Norbeck, S.O. Purvine, N.P. Manes, H.S. Smallwood, et al., Proteomic analysis of *Salmonella enterica* serovar Typhimurium isolated from RAW 264.7 macrophages identification of a novel protein that contributes to the replication of serovar typhimurium inside macrophages, *J. Biol. Chem.* 281 (2006) 29131–29140.
- [60] M.U. Shiloh, J.D. MacMicking, S. Nicholson, J.E. Brause, S. Potter, M. Marino, F. Fang, M. Dinauer, C. Nathan, Phenotype of mice and macrophages deficient in both phagocyte oxidase and inducible nitric oxide synthase, *Immunity* 10 (1999) 29–38.
- [61] N. Skunca, M. Bošnjak, A. Kriško, P. Panov, S. Džeroski, T. Smuc, F. Supek, Phyletic profiling with cliques of orthologs is enhanced by signatures of paralogy relationships, *PLoS Comput. Biol.* 9 (2013) e1002852.
- [62] O. Steele-Mortimer, The *Salmonella*-containing vacuole – moving with the times, *Curr. Opin. Microbiol.* 11 (2008) 38–45.
- [63] G. Storz, L.A. Tartaglia, OxyR: a regulator of antioxidant genes, *J. Nutr.* 122 (1992) 627–630.
- [64] D.J. Stuehr, Mammalian nitric oxide synthases, *Biochim. Biophys. Acta* 1411 (1999) 217–230.
- [65] J.A. Vizcaino, R.G. Cote, A. Csordas, J.A. Dianas, A. Fabregat, J.M. Foster, J. Griss, E. Alpi, M. Birim, J. Contell, G. O'Kelly, A. Schoenegger, D. Ovelheiro, Y. Perez-Riverol, F. Reisinger, D. Rios, R. Wang, H. Hermjakob, The Proteomics Identifications (PRIDE) database and associated tools: status in 2013, *Nucleic Acids Res.* 41 (D1) (2014) D1063–D1069 (PubMed PMID:23203882).
- [66] M. Wenk, Q. Ba, V. Erichsen, K. MacInnes, H. Wiese, B. Warscheid, H.-G. Koch, A universally conserved ATPase regulates the oxidative stress response in *Escherichia coli*, *J. Biol. Chem.* 287 (2012) 43585–43598.
- [67] C.C. Winterbourn, A.J. Kettle, Redox reactions and microbial killing in the neutrophil phagosome, *Antioxid. Redox Signal.* 18 (2013) 642–660.
- [68] C.C. Winterbourn, M.B. Hampton, J.H. Livesey, A.J. Kettle, Modeling the reactions of superoxide and myeloperoxidase in the neutrophil phagosome: implications for microbial killing, *J. Biol. Chem.* 281 (2006) 39860–39869.
- [69] C.C. Winterbourn, A.J. Kettle, M.B. Hampton, Reactive oxygen species and neutrophil function, *Annu. Rev. Biochem.* 85 (2016) 765–792.
- [70] Y. Yang, M. Hu, K. Yu, X. Zeng, X. Liu, Mass spectrometry-based proteomic approaches to study pathogenic bacteria-host interactions, *Protein Cell* 6 (2015) 265–274.
- [71] M. Zheng, Activation of the OxyR transcription factor by reversible disulfide bond formation, *Science* 279 (1998) 1718–1722.